

Influence of Laser Processing Parameters on the Corrosion Behavior in 316L Stainless Steel Laser Powder Depositions

Eswar R. Yarrapareddy^a, Alan J. Anderson, James W. Sears

Advanced Materials Processing (AMP) Center, South Dakota School of Mines and Technology, Rapid City, SD 57701, USA

1. Abstract

Laser Powder Deposition (LPD) is an advanced manufacturing process where metallic and/or ceramic powders are injected into a small molten pool produced by a focused laser beam. A computer-controlled robot controls the position of the molten pool, which allows for sequential layering that produces solid free form shapes directly from a CAD/CAM interface. The process parameters are implemented to control the molten pool size by changing the laser processing parameters (i.e. laser power, traverse speed and layer thickness). This work evaluated the corrosion behavior of laser powder deposited 316L stainless steels deposited at different laser processing parameters. The susceptibility of intergranular corrosion (IGC) of laser deposited 316L stainless steel bulk builds is studied by hot boiling sulfuric acid sensitization test. The pitting corrosion behavior of laser deposited 316L stainless steel thin walls is studied by cyclic potentiodynamic polarization methods. From this, the corrosion potential, and current density are calculated. These are related to laser processing parameters. The wrought 316L stainless steel is also tested for comparative study with laser deposited specimens. The laser deposited specimens are about 30% more corrosion resistant than the wrought materials.

2. Introduction

Laser Powder Deposition (LPD) is an advanced manufacturing technology used to fabricate near-net shape, fully dense metal components directly from a CAD/CAM interface without using traditional machining processes. The LPD system at Advanced Materials Processing (AMP) Center of South Dakota School of Mines and Technology (SDSM&T) consists of a high-power Neodymium Yttrium Aluminum Garnet (Nd: YAG) laser, a Fanuc M-16i six axis computer-controlled robot and two powder feeder units. The powder delivery nozzles are arranged to inject the powder streams directly into the focused laser beam.

A schematic representation of LPD system is shown in Figure 1. The system has a flat metal substrate generally made of the metal to be deposited. The laser beam is focused onto the metal substrate to create a molten pool and the powder delivery nozzles deliver the metallic or ceramic powders into the molten pool to increase the material volume. The computer-controlled robot controls the position of the molten pool. The system repeats the process over and over to deposit a layer of the structure. After one layer is deposited, another is deposited on top of it and so on. The system creates layer upon layer until it has produced a metal version of the CAD model¹. The movement of the laser controls the solidification of the molten pool. Typically the solidification rates are high, which produces fully dense materials with excellent mechanical and metallurgical properties. LPD has been shown to produce fully dense materials with properties equivalent or better than conventionally produced materials².

^a Author Electronic Mail: yereddy@yahoo.com

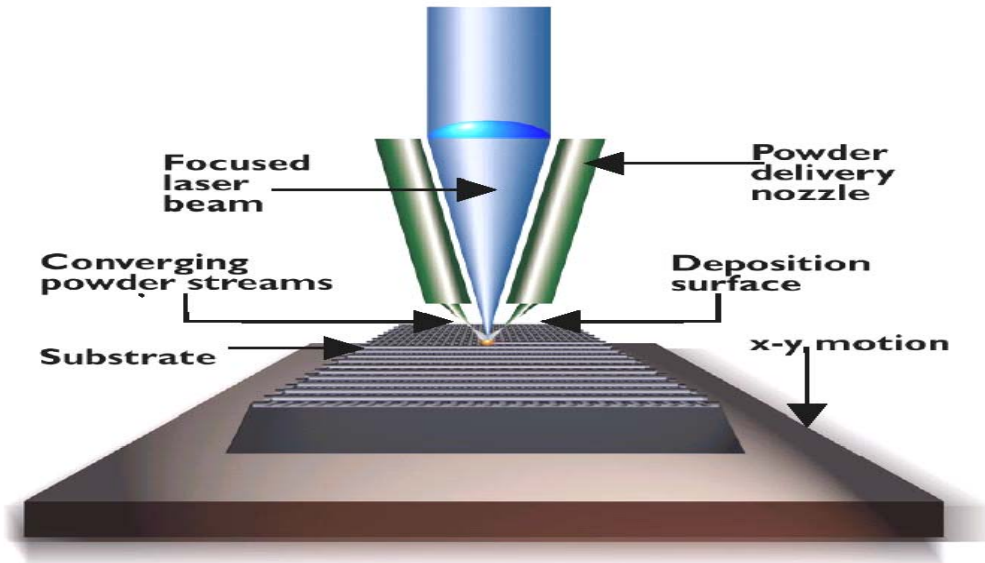


Figure 1. The schematic diagram of laser powder deposition.

3. Research Objective

The objective of this research is to investigate the corrosion behavior of laser powder deposited 316L stainless steels at different laser-processing parameters. The investigated corruptions are intergranular corrosion and pitting corrosion. These corrosion behaviors are studied in terms of laser-processing parameters. The parameters of interest are laser power, layer thickness, hatch width and linear velocity. For the current work only the laser power is varied, the layer thickness, hatch width and linear velocity are kept constant for all depositions. The laser processing parameters are interrelated, and this relationship is given by the specific energy as defined in the following equation.

$$\text{Specific Energy, SE} = (P_L \times \alpha) / (\text{BR}_{\max})$$

$$\text{BR}_{\max} = T_{ls} \times H_{hs} \times V_l \times 60$$

Where P_L is laser power

α is absorption coefficient

BR_{\max} is built rate

T_{ls} is layer thickness

H_{hs} is hatch width

V_l is linear velocity

Specific energy, as previously shown by Sears and Marchione, has an effect on the mechanical properties and microstructure of laser powder deposited 690N₂ material². In the current study the corrosion behavior is studied as function of specific energy, but since only the laser power is varied, the results are presented as a function of laser power only. However, it is important to note that this directly relates to specific energy in this case. The computer-controlled robot controls the position of the molten pool. The control of the molten pool size is predominately

influenced by the absorbed energy from the laser³. The chemical compositions of metallic powders used for depositing 316L SS and wrought 316L SS materials are given in Table 1.

Table 1. The chemical compositions of LPD metal powder and 316L wrought material

	C	Si	Mn	P	S	Cr	Ni	Mo	Fe
LPD-Metal Powder	0.019	0.50	1.44	0.022	0.007	16.5	10.20	2.09	Bal
Wrought 316L SS	0.03	1.00	2.00	0.045	0.003	18-20	12.00	2.00	Bal

4. Laser Powder Deposition Experimental Work

The 316L stainless steel (SS) bulk builds and thin walls are laser deposited by using Trumpf 3006L, 3 kW, Continuous Wave, and Nd: YAG laser. A Fanuc M-16i six-axis computer-controlled robot controls the laser-powder head motion. Two sample configurations are deposited: a bulk build and a thin wall build (see Figure 2 and 3). Four samples of each are made using the parameters in Tables 2 and 3.

The next part describes the corrosion tests used for this study, hot boiling sulfuric acid test is selected for detecting susceptibility to IGC and cyclic potentiodynamic polarization test is used to measure the resistance to pitting. Wrought 316L stainless steel material is also tested for comparative study. The laser powder deposited bulk builds are used for IGC testing and laser powder deposited thin walls are used for generating cyclic potentiodynamic polarization curves.

Table 2. LPD processing parameters for 316L SS bulk builds

Parameter	Sample 1	Sample 2	Sample 3	Sample 4
Linear Velocity (mm/s)	21	21	21	21
Hatch Width (mm)	0.75	0.75	0.75	0.75
Layer Thickness (mm)	0.50	0.50	0.50	0.50
Build Rate (cc/hr)	28.4	28.4	28.4	28.4
Specific Energy (watt-hr/cc)	19	23	26	30
Laser Power (watts)	550	650	750	850

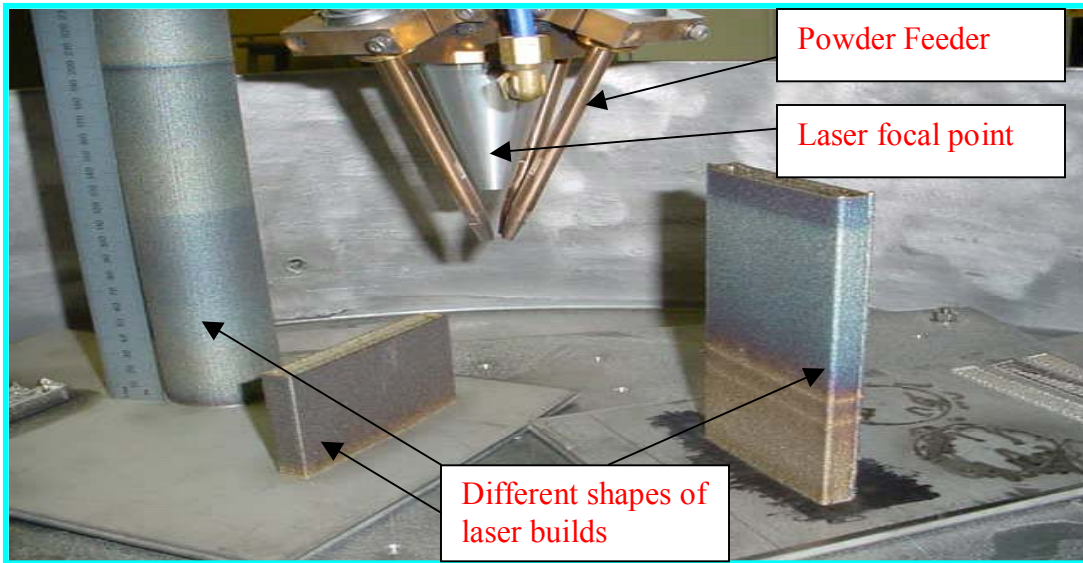


Figure 2. Examples of three builds along with the powder delivery nozzle aligned with the focused laser beam.

Table 3. LPD processing parameters for 316L SS thin walls

Parameter	Sample 1	Sample 2	Sample 3	Sample 4
Linear Velocity (mm/s)	21	21	21	21
Layer Thickness (mm)	0.50	0.50	0.50	0.50
Build Rate (cc/hr)	28.4	28.4	28.4	28.4
Laser Power (watts)	450	600	750	900



Figure 3. Example of 900 watts LPD processed thin wall structure.

5. Experimental Procedures

5.1 Hot Boiling Sulfuric Acid Sensitization Test

Four specimens (550, 650, 750 and 850 watts laser powder deposited) are sectioned from the top portion of laser powder deposited 316L SS bulk builds and a piece of 316L SS wrought material from 316L SS wrought material. All specimens are finished using different grit abrasive papers first, then fine polished with 1 μm and 0.05 μm abrasive solutions. The polishing is to remove any loose oxide layers that might be present on the surface of the specimens. The total surface area of these specimens is calculated including the edges. The polished specimens are placed in 1000 ml Erlenmeyer flask containing 600 ml of 50% reagent grade sulfuric acid and 25 grams reagent grade ferric sulfate. These specimens are heated for 120 hours as per ASTM G28-97 standard method⁴. The experimental set up of hot boiling sulfuric acid sensitization test is shown in the Figure 4.

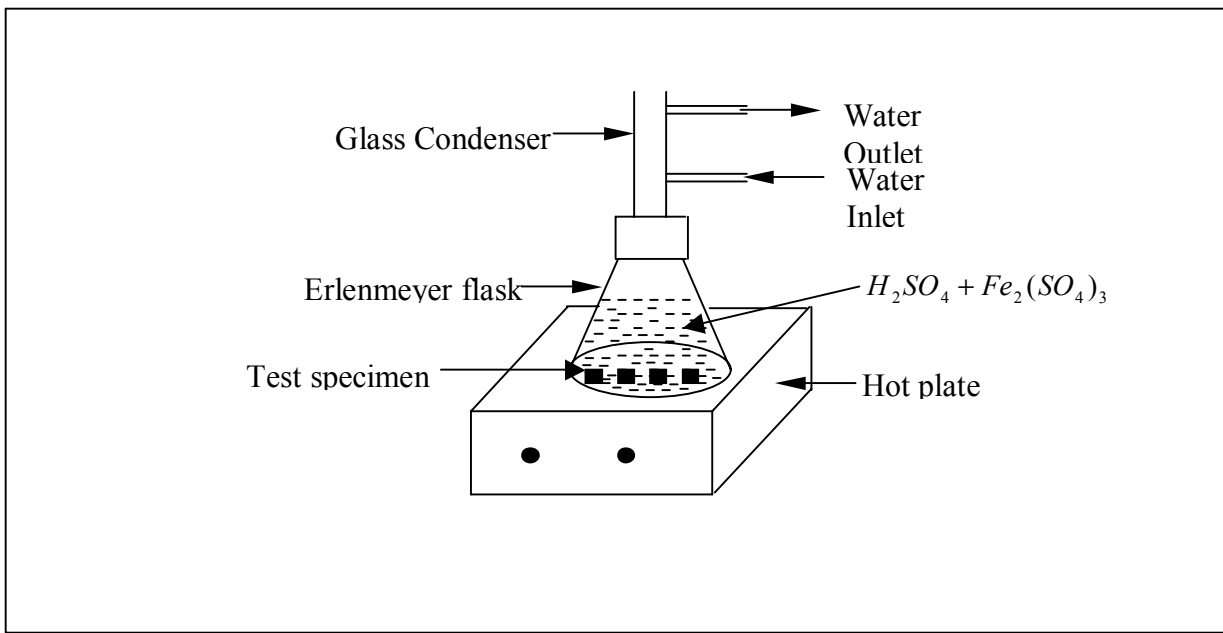


Figure 4. The schematic representation of hot boiling sulfuric acid sensitization test

5.2 Cyclic Potentiodynamic Polarization Test

Laser powder deposited thin walls (600, 750 and 900 watts) are sectioned into 30x30 mm specimens. A 30x30 mm wrought 316L SS is also sectioned from 316L SS wrought plate. These specimens are first rough polished then fine polished. The polishing is intended to remove any loose oxide layer that might form on the surface and to minimize the effect of surface roughness⁵. Potentiodynamic polarization tests are conducted on computer-controlled model 273 EG&G potentiostat as per ASTM G 61-86 standard test method⁶ to study the pitting corrosion behavior. Polarization curves are generated in 3.5% deaerated NaCl solution at room temperature. The NaCl solution is deaerated by purging nitrogen gas for about one hour. The potentials are measured with respect to standard saturated calomel electrode ($E_{SCE}=0.242$ Volts). Sintered platinum electrode is used as a counter electrode and the test sample served as working electrode. 5 mV/s scan rate is used during the polarization tests. The specimens are immersed in

the test solution for one hour before the polarization. The potential, total current and time are continuously monitored. From these polarization curves the corrosion potential, pitting potential and current density are calculated. The experimental set up of potentiodynamic polarization test is shown in the Figure 5. All experiments are conducted at an ambient temperature of 24⁰C.



Figure 5. Potentiodynamic polarization test experimental set up.

6. Results and Discussions

6.1 Hot Boiling Sulfuric Acid Sensitization Test

The effect of the acid solution on specimens was calculated using the following formula⁶.

$$\text{Corrosion Rate} = (K \times W) / (A \times T \times D)$$

Where K = A Constant = 3.45×10^6

T = Time of exposure, h, to the nearest 0.01 h

A = Area, cm², to the nearest 0.01 cm²

W = Weight loss, g, to the nearest 0.001g and

D = Density, g/cm³

The measured weight loss and the corrosion rate values are summarized in the Table 4. The presence of IGC is determined by comparing the measured corrosion rate values. The specimens deposited at higher laser power are more IGC resistant than the specimens deposited at lesser laser power. 650, 750, 850 watts laser deposited specimens corrosion rate values are lying in the good relative corrosion resistance range and 550 watts laser deposited sample and wrought 316L SS sample lying in the fair range as shown in the Table 5. The relationship between the corrosion rate values and laser power are plotted in the Figure 6. The intergranular corrosion attack can be seen in between the layers in laser deposited specimens and around the grain boundaries in wrought material. The IGC attack in between the grain boundaries in laser deposited specimens and wrought materials is shown in SEM microstructures in Figure 7. The laser powder deposited specimens are about 30% more corrosion resistant than the wrought materials.

Table 4. Corrosion rate values for different specimens

Laser Power (watts)	Weight Loss (grams)	Total Surface Area (cm ²)	Corrosion Rate (mpy)
550	0.1925	25.18	26.488
650	0.1436	25.64	19.405
750	0.1407	27.14	17.962
850	0.1221	25.49	16.596
Wrought 316L SS	0.1868	26.14	24.760

Table 5. Comparison of corrosion rate with relative corrosion resistance⁷

Relative Corrosion Resistance	Corrosion Rate in mpy
Outstanding	<1
Excellent	1-5
Good	5-20
Fair	20-50
Poor	50-200
Unacceptable	200 +

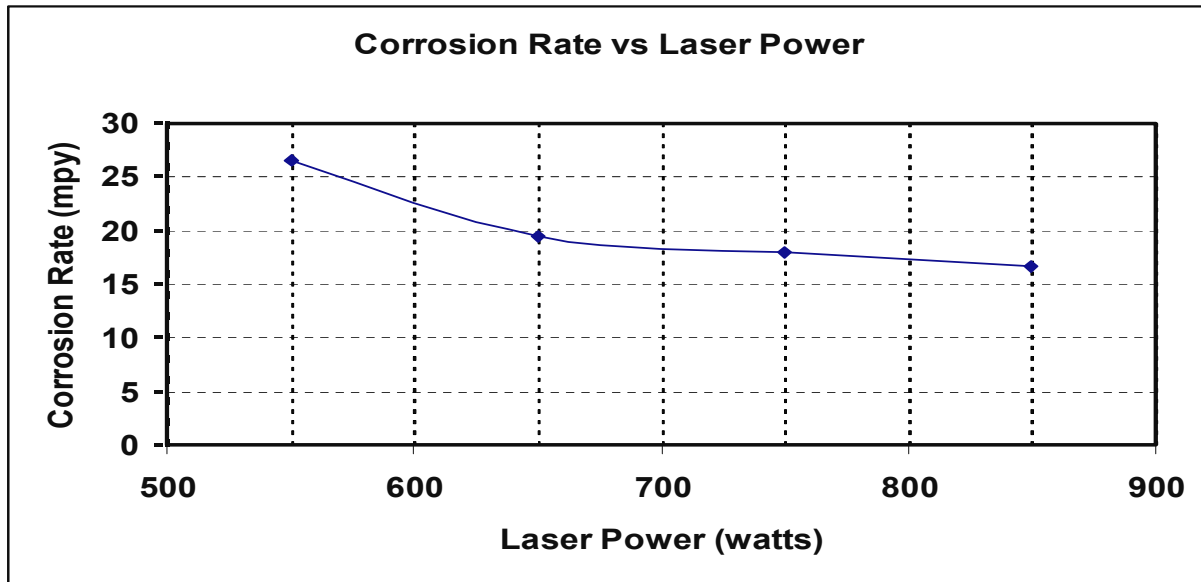


Figure 6. Relationship between corrosion rates vs. laser power.

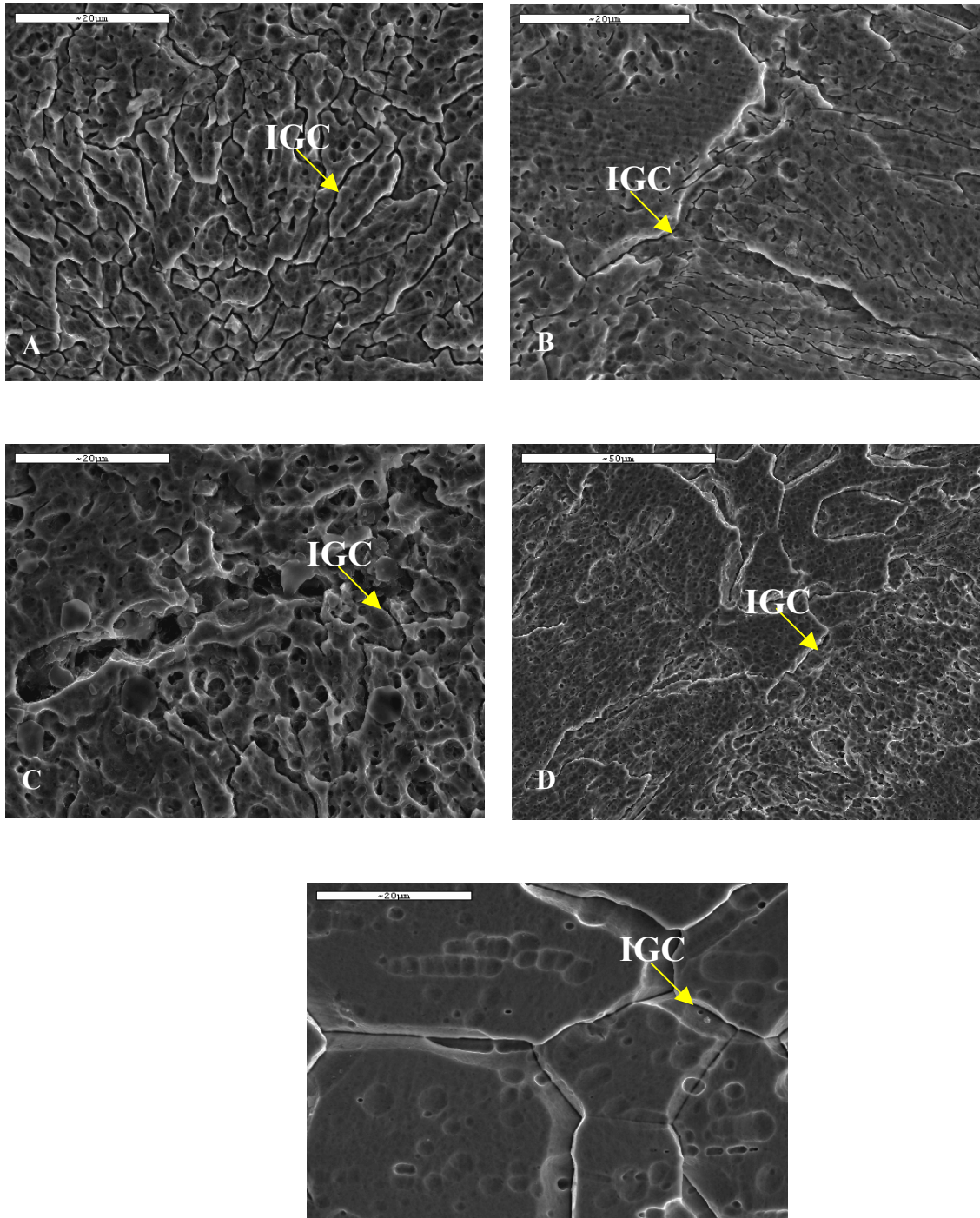


Figure 7. SEM microstructures of laser deposited 316L SS specimens of laser power 550 (A), 650 (B), 750 (C) and 850 (D) watts and wrought 316L SS (E) after hot boiling sulfuric acid test.

In stainless steels the IGC is mainly due to the impoverishment or depletion of chromium in the grain-boundary areas¹⁰. The addition of chromium to ordinary steel imparts corrosion resistance to the steel in many environments. Generally more than 10% chromium is needed to make stainless steel. If the chromium is effectively lowered, the relatively poor corrosion resistance of ordinary steel is reproduced. The carbon diffuses towards the grain boundary quite faster at sensitizing temperatures, but chromium is much lesser mobile. The 17% chromium that is present in 316L stainless steels will be depleted in grain boundary regions resulting in the intergranular corrosion⁷.

In the case of 316L SS, there is very low carbon, so sensitization is generally not a problem; thus the improvement in the LPD specimens is due to another effect. It is hypothesized that the high cooling rates results in a fine microstructure with very little segregation and improved IGC resistance. It is noted that the lower laser powers result in finer microstructure and many more grain boundaries. It is expected that the number of grain boundaries will decrease as laser power increases resulting in improved IGC resistance. It is also hypothesized that the ferrite content decreases as laser power increases thereby decreasing the susceptibility to IGC.

6.2 Cyclic Potentiodynamic Polarization Test

The potentiodynamic polarization curves for the laser deposited 316L SS and 316L SS wrought material are shown in the Figure 8. These curves clearly indicate the specimens deposited at higher laser power have higher corrosion potentials and the specimens deposited at lesser power have lesser corrosion potentials. The corrosion potentials for different specimens are summarized in the Table 6. The current densities are calculated by drawing tangents to the anodic and cathodic curves, where there is a sharp increase in the potential, and extrapolating the tangent's intersection point onto the x-axis. The calculated current densities are summarized in Table 7. These show the lower laser power deposited specimens are less pitting corrosion resistant and higher laser power deposited specimens are more pitting corrosion resistant.

The graphs showing the relationship among corrosion potential, current density and laser power are shown in the Figures 8 and 9. The potential at which the current sharply increases is defined as the pitting potential. The potential up to which we can protect the material from pitting is called protection potential. If the pitting potential and protection potential are the same, there will be little tendency to pit. If the protection potential is more positive (anodic) than the pitting potential, there will be no tendency to pit. If the protection potential is more negative than the pitting potential, pitting could occur⁸. There might be two possible reasons for the improved pitting resistance after laser powder deposition: (i) less segregation the major alloying elements Cr and Ni, or (ii) suppression or elimination of inclusions by high cooling rates⁹.

In summary, potentiodynamic polarization curves are useful in studying the localized corrosion such as pitting corrosion. This describes how material will behave when exposed to particular liquid environment. This test procedure also indicates the ability of the specimen to protect itself against aggressive attack from the liquid environment.

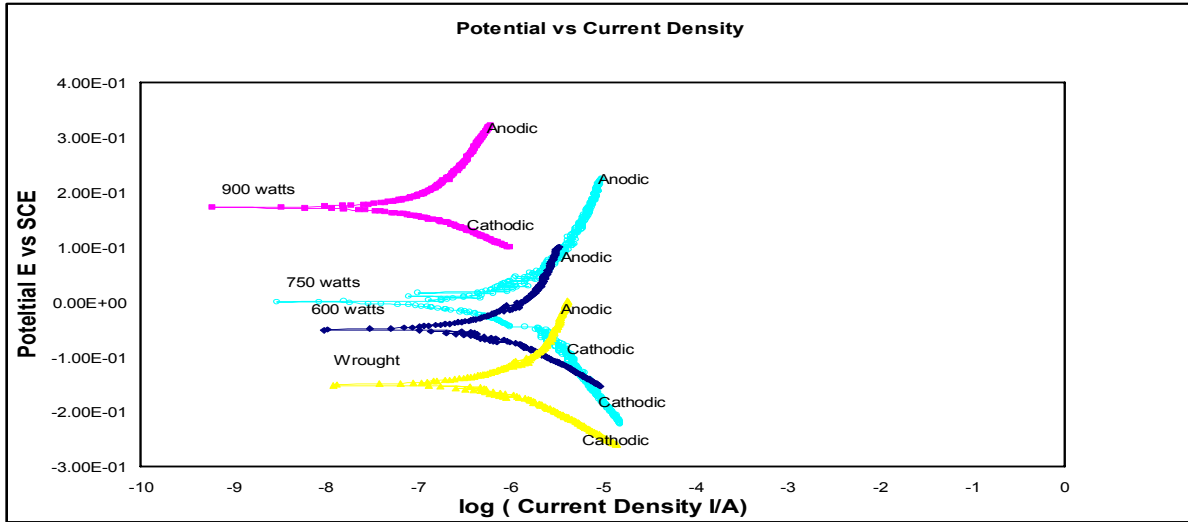


Figure 8. Potentiodynamic polarization curves for different LPD thin walls.

Table 6. Corrosion potentials for different laser deposited 316L stainless steel specimens

Laser Power, watts	Corrosion Potential, mV
Wrought 316L SS	-151
600	-52
750	0
900	172

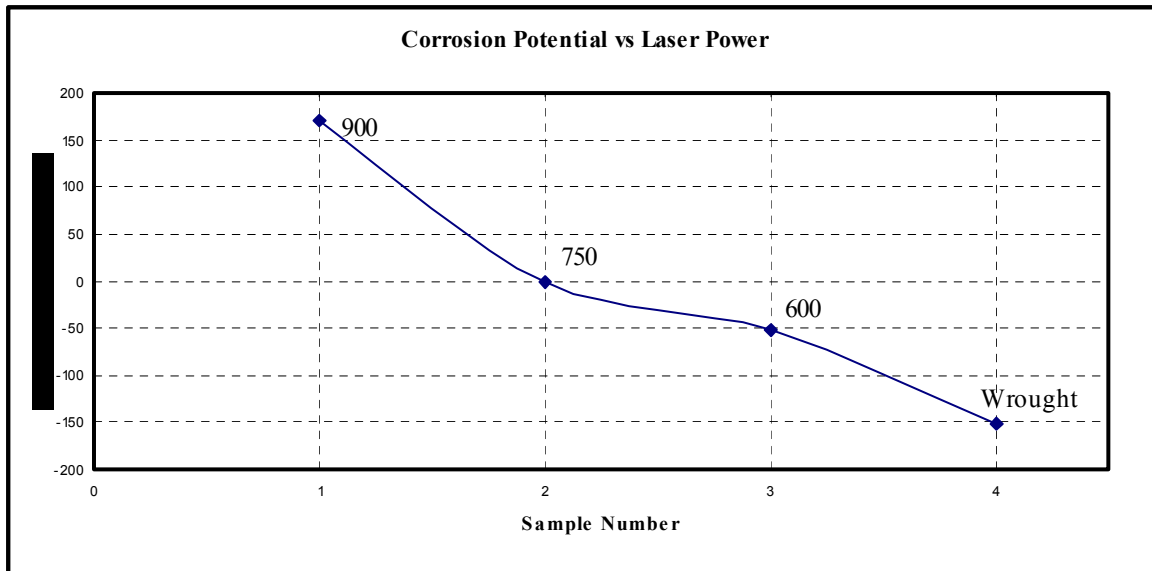


Figure 9. The relationship between corrosion potential and laser power.

Table 7. Current densities for different laser deposited specimens

Laser Power, watts	Current Density, nA/cm ²
Wrought 316L SS	603
600	501
750	355
900	89

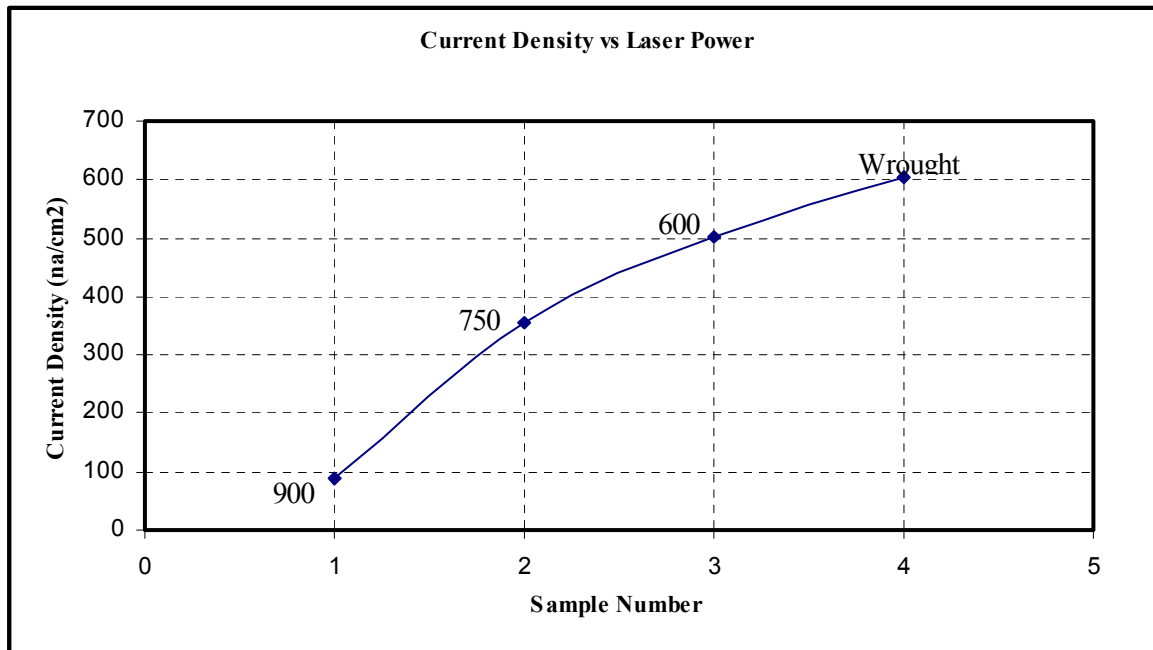


Figure 10. The relationship between current density and laser power.

7. Conclusions and Future work

7.1 Conclusions and Discussions

The laser powder deposited 316L stainless steels with higher laser power are more IGC resistant than the specimens deposited at lesser laser power and 316L stainless steel wrought materials. In fact, the 850 watts laser deposited specimen is about 30% more IGC resistant than 316L stainless steel wrought materials. The possible reasons for the improved IGC resistance might be that as the laser power increases grain size also increases and lesser total grain boundary area will be available for IGC attack. Another possible reason might be, as the laser power increases there might be decrease in the percentage of ferrite content in final product, if we assume the ferrite phase plays major role in IGC attack. It is also hypothesized that the high cooling rates results in a fine microstructure with very little segregation and improved IGC resistance. It is noted that the lower laser powers result in finer microstructure and many more grain boundaries. It is also

expected that the number of grain boundaries will decrease as laser power increases resulting in improved IGC resistance.

The corrosion potentials of laser powder deposited specimens are moving more towards the noble direction as the laser power is increasing. The pitting corrosion resistance of laser powder deposited specimens deposited at higher laser power is higher than that of laser powder deposited specimens deposited at lesser laser power and wrought material.

In summary, the laser powder deposited specimens give about 30% improvement in corrosion rate over the conventional wrought materials. This would demonstrate that the laser powder deposition gives improved corrosion resistance materials over conventional wrought materials. This improvement in the corrosion resistance will improve the longevity of the materials used for different applications. The current results are in agreement with Optomec LENS-deposited 420 stainless steel results¹⁰.

7.2 Future Work

The future work may include:

1. X-ray diffraction analysis to identify and quantify the phases present before and after testing specimens for hot boiling and potentiodynamic polarization tests. This work will tell us what phase is mainly corroding.
2. Quantify the grain boundary surface area to show that it changes with laser power. This will support the hypothesis that some of the increase in corrosion resistance is caused by the decrease in grain boundary surface area.
3. Investigating the other types of corrosion behavior of laser deposited specimens and comparing the results with wrought materials.

8. Acknowledgements

This work is fully supported by U.S. Army Research Laboratory and U.S. Army Office under the grant number DAAD 19-02-2-001. Support from the infrastructure of AMP Center and Department of Materials and Metallurgical Engineering of SDSM&T is also acknowledged. The authors would also like to thank Mr. Bill Arbegast and Dr. Glen Stone for their invaluable suggestions.

9. References

1. Richard Grylls., "Laser Engineered Net Shapes" in *Advanced Materials & Processes/* January 2003, Volume 161, No.1, PP 45-46.
2. Sears, James W. and Marchione, Thierry, "The Effects of Processing Parameters on Microstructure and Properties of Laser Deposited PM Alloy 690N₂ Powder", 2002 International Conference on Metal Powder Deposition for Rapid Manufacturing.
3. Sears, James W. and Marchione, Thierry, "Issues in Increasing Builds Rates for Laser Deposited PM Alloy 690N₂", *Proceeding of the 2003 International Conference on Powder Metallurgy and Particulate Materials*, June 8-12, 2003 Las Vegas, NV.
4. ASTM Standard G 28-97 "Standard Test Methods of Detecting Susceptibility to Intergranular Corrosion in Wrought, Nickel-Rich, Chromium-Bearing Alloys".
5. K.H. Lo, C.T. Kwok, F.T. Cheng, H.C Man., "Corrosion resistance of Laser-Fabricated Metal-Matrix Composite Layer on Stainless Steel 316L" *Journal of Laser Applications* Vol.15 No.2 May 2003, pp107-114.

6. ASTM Standard G 61-86 "Standard Test Method for Conducting Cyclic Potentiodynamic Polarization Measurements for Localized Corrosion Susceptibility of Iron-, Nickel-, or Cobalt Based Alloys".
7. Corrosion Engineering by Mars G. Fontana, Third Edition, PP 172-173
8. EG&G Princeton Applied Research, Electrochemistry and Corrosion Overview and techniques Laboratory Manual, P 9.
9. E. McCafferty and P.G. Moore, "Corrosion Behavior of Laser-Surface Melted and Laser-Surface Alloyed Steels", Journal of Electrochemical Society, Volume 133, No.6, June 1986.
10. Optomec-Laser Engineered Net Shaping Technical Brief on 'Improved Corrosion Resistance of LENS 420 SS' PP 1-4.